A climatology of IASI radiances spectra to monitor global climate change

Thierry Phulpin*, Sebastien Gaugain and Joachin-Pedro Gonzalez

*TIRSEC, 6bis chemin de Mange-pommes, 31520 Ramonville, France
CNES 18 avenue E. Belin, 31401 Toulouse cedex France

Abstract
Infrared spectra from IASI on Metop have the quality to be used in climate monitoring. As IASI and its successor are planned to fly for more than 30 year there is potential to exploit its capability for estimating long term trends. In this paper we show the first results of a climatology based on statistics of the spectra at scales of months to years and at global scale. Some proxies are found in the spectra to monitor the time variations of some important climate variables. An inversion of annual gradients has been performed giving results very close to those obtained from National Climatic Data Center(NCDC) statistics, confirming the pertinence of the approach. A comparison of month by month spectra shows *inter-annular differences that can be related to climate events.*
IASI also offers the possibility to monitor consistently several variables over the globe. Applications at regional scales, for example, over tropical oceans and the Antarctic have started.
.

Introduction
Satellite data are generally considered as of prime importance for climate monitoring. However climate modellers need very long time series (30 years at least) of very precise measurements to assess the results of the models. Only recurrent meteorological satellites are able to provide such long data series. Generally, the confrontation of satellite and models is performed through comparison of Essential Climate Variables (ECV), which for the satellite are level 3 or 4 products resulting from inversion or assimilation methods (ref). Each variable being retrieved separately, the consistency between the ECV is generally not considered resulting in some uncertainty in the analysis.
. Only re-analysis provides some consistency through the model which funds the models. But re-analysis outputs need also to be confronted with satellite measurements.
The potential for climate monitoring by using satellite infrared radiance spectra has been shown in some previous studies [e.g. Brindley and Harries, 2003, Brindley and Allan,, 2003]. The interest of using IASI level1 spectra is justified by the long duration of the IASI programme, the very high quality of the data and the wealth of information content in the spectra. The IASI products contains information on cloud cover, on the atmospheric temperature and humidity, on surface temperature and surface emissivity and on total columns of CO_2, CO, CH_4, O_3 and others (e.g. Hilton et al, 2011) . The integrated radiance is also strongly related to the outgoing longwave radiation (OLR). Climatology of IASI level 1 spectra is thus expected to deliver some information on the relation between the climatic events and the change in consistency of the variables to which the spectra are sensitive. Using IASI radiances only prevents any dependency on the models which generally appears in inversion process to get level 2 products.
In this paper we first describe IASI, the programme, the instruments, its performances and the level 1c products. In the section 2, we describe the climatology which has been started with almost 4 years of IASI on Metop-A. Representativity of the statistics are discussed in section3. Mean monthly global spectra for clear/cloudy conditions, night/day, land./sea have been computed. The mean radiance (or brightness temperature) summed over all wavenumbers and viewing angles is strongly related to the OLR. Its variations along 35 months are shown and interpreted in section 4. In section 5, simulations of IASI spectra are performed with 4A/OP Radiative transfer code (ref) , using the more representative atmosphere of global cloud free conditions. The Jacobians with respect to various variables are also computed. In section 6, the average global annual spectra are computed and simple inversion based on the Jacobians computed previously is performed. The year to year change for the various ECVs is exhibited and interpreted in relation to Nina events in 2010 and 2011. To go deeper into details, the monthly anomalies in spectra (referred to the total mean) are analyzed. IASI spectra can also be used for regional climatology.

2. IASI Level 1 data
IASI-A was launched on Metop-A in September 2006 but first data were released in June 2007. Since then IASI, a Fourier Transform Spectrometer designed by CNES and developed in cooperation with Eumetsat (Chalon et al., 2001), measures outgoing infrared radiance spectra from 645 cm^{-1} to 2760 cm^{-1} with 0.25 cm^{-1} spectral sampling. There are 30 views across track from -48.3 to 48.3 degrees, each field- of- regard containing a set of 4 pixels of 12 km at nadir (Figure 1). The data quality operationally monitored by CNES has proven the very high stability of the measurements and their very high radiometric spectral and geometric accuracy (Blumstein et al., 2007).

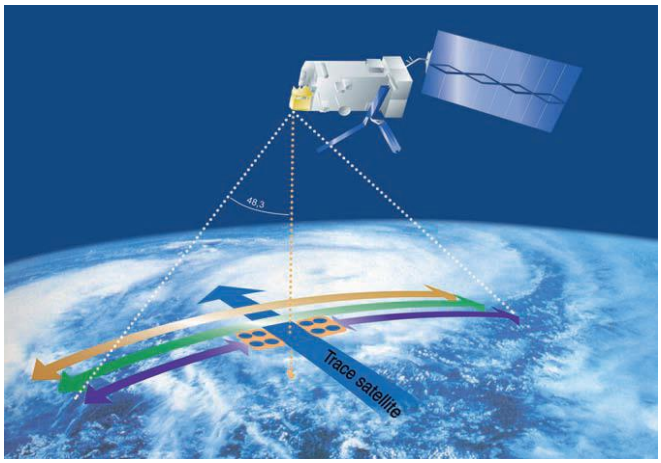

Figure 1: Geometry of IASI

For climatic studies the prior interest of IASI is two-fold: the duration of the programme is at least 15 years with 3 similar instruments which are planned to be intercalibrated. IASI-B on Metop-B was launched in October 2012. After 2020, the follow-on, now designed, will be IASI-NG with improved radiometric performances and spectral resolution (a factor 2), but covering exactly the same spectral range and with a quite consistent geometry (same orbit, same scan). This is a boon to make statistics over a long period of time (more than 30 years) and study trends at middle term.
The second advantage of IASI is the spectral domain covering the main absorption bands of atmospheric gases CO_2, H_2O, CH_4, N_2O, O_3, also trace gases like CFC or SF_6 or HNO_3, and allowing temperature profiles retrieval. Indeed, it allows us to monitor all these variables consistently and study correlations between them and time lag to propagate at various atmospheric levels.

Level 1 processed data are available from Eumetsat either in near-real time (through Eumetcast infrastructure for Europe) or from the U-Marf archiving system. Global data, all processed with the same software, are available twice a day. Information in level 1 contains full spectra (8461 channels) in all pixels, ancillary data like solar zenith angle and information on surface types in each pixel given by the 1km resolution AVHRR imager data segmented in the IASI pixels.
Last upgrade of processing was performed in June 2010. Since then the Level1C product includes AVHRR cloud fraction in IASI pixels.

3. Average spectra and representativity

For sake of simplicity, the spectra in radiance are averaged for all viewing angles and all lines and pixels along the orbit. Typical values of total number of pixels in a month are around 40 millions. Variations of the number of pixels by box of 2° by 2° are represented in figure 2. It appears that there is an oversampling of latitudes between 70 and 85° which is due both to the orbit inclination and the scan width. This is repeated every day and will not affect trend analysis. In addition a slight deficit of points is observed in the South Atlantic anomaly zone. This deficit has a very small impact generally lower than 0.04K on the global average spectra.

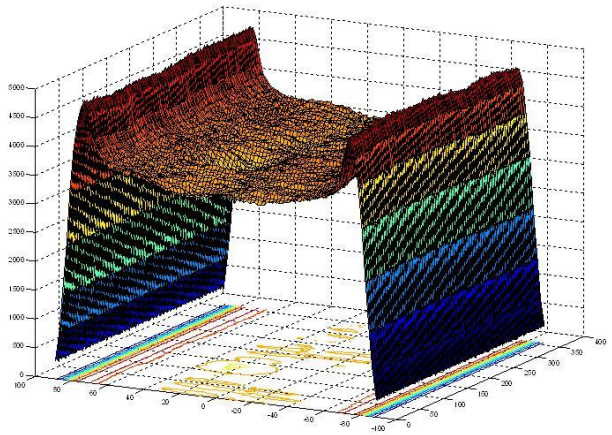

Figure 2: Distributions of number of pixels along latitude and longitude in a 2° by 2° grid.(Mercator?)

The statistics provide for each of the 8461 IASI channels, respectively for all pixels, for cloud free and cloud overcast pixels, the mean radiance, its standard deviation, the skewness and kurtosis. They are produced separately for all pixels, for cloud free pixels (AVHRR cloud fraction =0) and supposed overcast pixels (cloud fraction >0.95). Separate statistics are computed for daytime data (local sun zenith angle <90°) or night time, and also for ocean or land pixels. The radiances are converted in brightness temperature at the end of the processing. It is more 'physical' to sum up radiances than temperatures. Nevertheless the final difference is small and can be approached using Taylor's expansion.

Average monthly mean spectra can also be used to check stability and quality: a comparison of IASI-A mean spectra with IASI-B in the first months of calibration/validation shows a very good consistency with a bias lower than 0.1 K over the full spectral domain. Nevertheless this bias cannot only be subtracted when replacing IASI-A by IASI-B in the climatology, since there is also a monthly variability of this bias. A model has to be defined to allow intercalibration with mean error lower than 0.02C.
The cloudfree or cloudy statistics for IASI-B also exhibit a significant bias compared to IASI-A. This is due to the use of miscalibrated AVHRR channel 5 of Metop-B in the cloud test generating a higher cloud fraction in the level1C IASI-B products.

4. Outgoing LW radiance estimate from IASI spectra

Regarding the total outgoing longwave irradiance the spectral domain covered by IASI (645 to 2760 cm^{-1}) corresponds to about 2/3 of the total flux. The missing contribution is the one from 50 cm^{-1} to 645 cm^{-1} which is mostly covered by water vapour lines.
Irradiance is also the integral of all directions, when IASI measures only from +/- 48.3°.(Lost fraction?) Nevertheless the integral over all the angles and all IASI spectra can

reasonably be considered as a first estimator of the outgoing (at the top of atmosphere) longwave radiation (OLR). Plots for the 'all' pixels (a predictor of the OLR) and only for the cloud free pixels somehow related to the surface radiation are shown on figure 3.
Main observations are the lag between the two cycles. Surface radiation is maximum in July-August and minimum in December-January while OLR would be maximum in October and minimum in May. The latter is much less variable than the first. Note that the corresponding brightness temperature (the mean of the spectra) varies in the year between 257 and 259 K. The global clear infrared flux is higher in 2012 than in 2011, OLR is slightly higher in 2011. I think you need to discuss prior measurements of this quantity. Reviewers are bound to pick this up so ISCCP and other estimates of OLR need to be mentioned and referred to here.

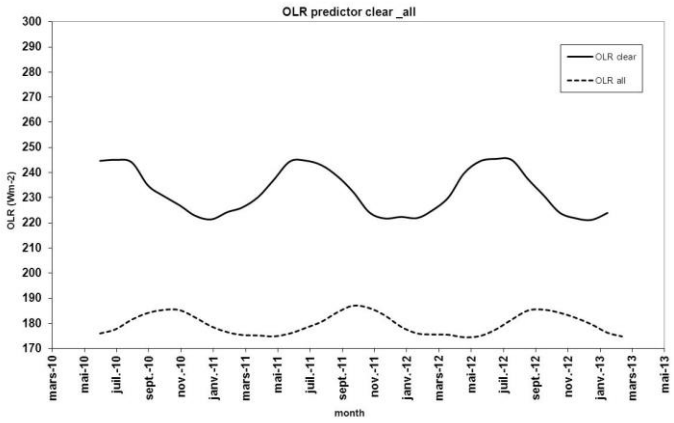

Figure 3: Estimator of the Global Outgoing longwave radiation (OLR) for all the IASI pixels or for the cloudfree pixels only from June 2010 to March 2013.

5. IASI Spectra simulation and sensitivity to variables
IASI spectra are simulated with the 4AOP radiative transfer code (Chaumat et al, 2006). The profiles which are given for the simulation are a mean tropical profile, midlatitude summer profile, midlatitude winter, subarctic summer and subarctic winter based on the profiles from the Tigr-2000 database (ref). The Instrument response function ISRF is the Level 1c with 0.25 cm^{-1} spectral sampling. The simulation has been first performed for the 15 viewing angles of IASI. The average of the spectra for all the 15 angles is equivalent to spectra at 30° with acceptable error lower than noise in most of spectral regions but those where spectral variations are sharp and where the signal can saturate due to the increase of path length for angles (Figure 4).
The simulated spectra are then computed only for this viewing angle of 30°.
Sensitivity of the spectra to various parameters has been computed by varying them separately. A plot of the sensitivity is given in figure 5 for the mean tropical atmosphere of Tigr-2000 database.
This plot shows that there are spectral regions which are only sensitive to restricted number of parameters where these parameters could be retrieved. The wealth of information is huge. A list of the main significant regions of the spectra is given in the table 1.

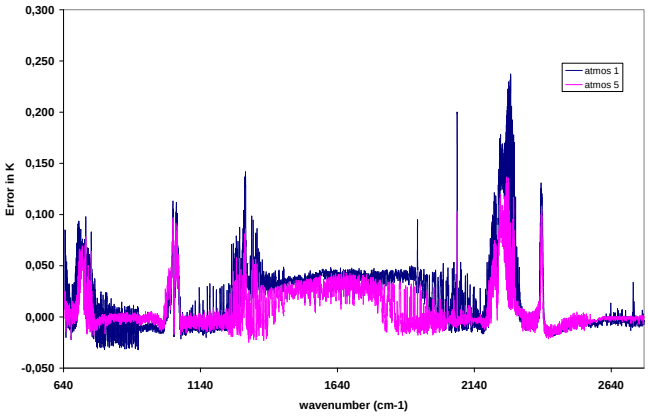

Figure 4 : Simulated discrepancy between spectra averaged over all IASI viewing angles and spectra under 30° viewing angle for 2 mean atmospheric conditions (resp. tropical and midlatitude winter)

Nevertheless, the information content cannot be restricted to the list of indicators in the table, since many other variables can also be of interest, some known (for example CFCs or HDO), some not yet identified and conserving full spectra content is deemed better for further exploitation. On top of that, the mean full spectra can be used as reference for calibration control, analysis of data quality and intercomparison with other sensors (among them next IASI or IASI-NG).

5. Statistics for years 2010 to 2013
The monthly mean spectra of IASI were computed from June 2010 to January 2013. The time series begins only in June 2010 because before that the cloud fraction used to flag cloud free pixels and overcast pixels was not available. This cloud fraction is derived from AVHRR 1 km resolution channels **(**see definition in IASI L1 PPF evolution for Day-2", ref EUM/OPS-EPS/SPE/08/0231).

5.1 The statistical distribution
Statistics can be interpreted in terms of climate variations if the average values of the measures are linked to the state and variations of given (Essential) climate variables. This means that quantities to be used identified as 'indicators' or proxies are strongly connected to a given variable (unambiguously). Also, the average should reflect the average of this variable, without distortion due to the (time and geographic) sampling. The average is meaningful if statistical distribution is quasi-gaussian. This can be characterized by the skewness and kurtosis. As an example, the geographic distribution must be well balanced to avoid that change in regions over- or under-represented affect annual variations. In addition, variations resulting from sampling conditions related to the cloud cover distribution must be identified.

Spectral range or wavenumber (cm^{-1})	Quantity	Variable
645-2760	Sum of radiances	Estimator of OLR
	Min value	Proxy of tropopause temperature
	Max value	Proxy of surface emission temperature Limited at 2100 cm^{-1} during daytime
667.75	Tb	Estimator of upper stratosphere/mesosphere Temperature
645-718		CO_2 and stratosphere mean Temperature
721-800		CO_2 and tropospheric Temperature profile
800-1000	slope	Clear sea : continuum absorption Land clear : emissivity + aerosol Cloud : liquid or ice
790-805		
940-980	Tb	XCO_2
1020-1070	Tb	Total Ozone
1070-1220	Slope	
1120- 1210	Tb	Water vapour profile
1150-1225	Tb in lines	H_2O Total column
1290-1310	Tb	XCH_4
1350-1440	Slope and Tb	Low Troposphere Temperature or stropsheric water at some lines
1900-2000	id.	Id
2115-2125		O_3
2150-2190		CO/H_2O
2190-2240		N_2O
2240-2290		CO_2 troposphere
2290-2390		CO_2 high atmosphere
2500-2590		N_2O
2741.5		CH_4
2600-2760	Slope and Tb	Ts , emissivity and HDO

Table 1: regions of spectra and characteristics related to main variables detected by IASI

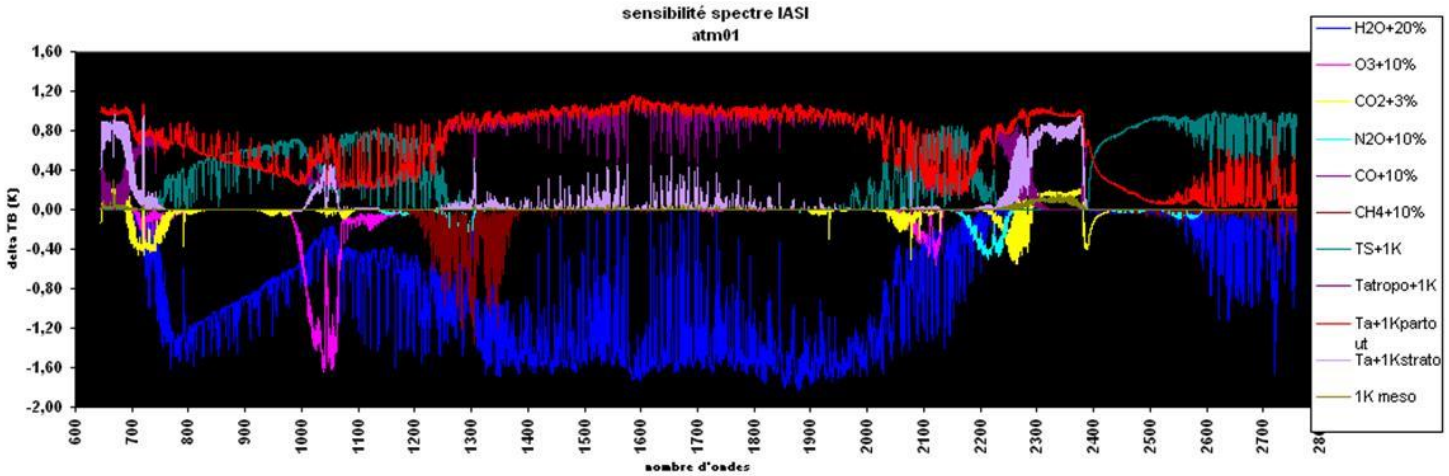

Figure 5: Sensitivity in Tb to separate variations of several variables: Ts (1K), T (1K) in troposphere, Stratosphere and mesosphere, absolute humidity (20%), CO_2 (3%), CO (10%), CH_4 (10%), N_2O (10%), O_3 (10%)

For cloud cover, the statistics in cloud free conditions are strongly dependent on the accuracy of cloud detection. While the IASI radiances produced by the level 1 processing are not to be reprocessed frequently, the algorithm defining the cloud fraction in the pixel can potentially be upgraded during the programme's life.

5.2 Cloudiness

AVHRR cloud fraction in the IASI pixels has been analyzed. The variations along the year and on the full series are very small. The average is around 0.65 +/- 0.02 fluctuations (Figure 6). This is close to the values obtained by the GEWEX cloud assessment (Stubenrauch, 2012). This gives a reasonable confidence in the cloud mask included in the Level 1c products since June 2010. The weakness is mostly the dependence on the good calibration and stability of AVHRR. The number of cloud contaminated IASI pixels monthly over the globe is very stable around 85.5%, i.e; the number of totally cloudfree is very stable each month around 15%. Similarly the number ou fully overcast pixels is very stable at global scale around 42%.

Comparison for sea/land and for day and night shows that cloud cover over the sea is almost constant (around 70%) and more variable between day (9:30 LST) and night (21:30 LST) over land. On the average the higher values are over the oceanic areas.

5.3 Reflected sun irradiance

Impact of reflected sun radiation affects spectra during daytime from 2500 cm^{-1} to 2760 cm^{-1}, a spectra domain where the atmosphere exhibits very transparent micro windows which can be used to retrieve surface temperature. The solar reflection effect can be approached by a linear equation the slope of which is related to the mean reflectance of the target. Accurate correction of this additional contribution to the surface radiance is possible. Nevertheless in this study the window is only used in night time acquisitions (Sun zenith angle lower than 90°) to get sea surface temperature.

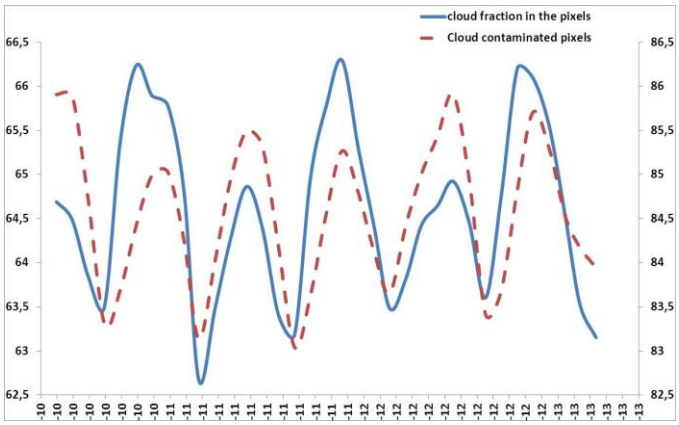

Figure 6: Monthly global means of cloud fraction in IASI pixels (full line) and ratio of IASI cloud contaminated pixels (dotted line) from June 10 to April 13

5.4 Indicators or proxies

The mean value over the spectral range is a proxy of the outgoing longwave radiation . The maximum (at 2143 cm^{-1}) if sun contaminated part of the spectra is excluded) is seen as a proxy of the surface temperature. In the case of night time data over the ocean the maximum is at 2700.75 cm^{-1} and is a very accurate estimate of the actual sea surface temperature (ref?). The minimum brightness temperature is measured at 686.5 $cm^{-1}$and is a fairly good indicator of the tropopause temperature. Brightness temperature at 667.75 cm^{-1} gives an estimate of the temperature around 5 hPa and is a characteristic of the spectra For the atmospheric gases: water vapour, ozone, carbon monoxide, methane and carbon dioxide, the technique is a normalized difference between the brightness temperature in the deep absorbing lines and and ones as close as possible to a window on the edge of these lines. The pairs of channels for the various gases are given in table 2. For the total water vapour column the technique is the same but the difference is here computed between the sum of brightness temperature in the absorbing band and the surface temperature estimated at 2183 cm^{-1} (all) or 2700.75 cm^{-1} (sea).

Species	Absorption/window
Ozone	1056.25 or 1034.75/1079.25 cm^{-1}
Methane	1292.5/1291.71 cm^{-1}
Carbon dioxide	948.25 or 976 / interpolated transparent
Carbon monoxyde	2161.75/2143 cm^{-1}
Water vapour (H2O)	1163-1213cm^{-1}/2143cm^{-1}
(HDO)	2619-2739/2143cm^{-1}

Table 2: Pairs of channels used to estimate proxies of trace-gas columns.

For the SST and the Total water vapour column, a comparison with ERA Interim products (ref) was performed showing that relative time variations of the indicators reflect very well the one from ERA Interim, demonstrating the pertinence of these proxies. For example, Figure 7 illustrates the good correlation of the IASI SST proxy with monthly mean of SST in the tropical ocean given by ERA Interim.

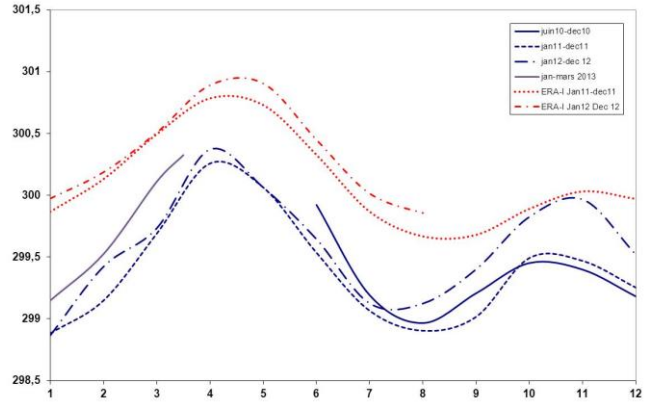

Figure 7 : Comparison of SST from ERA-Interim (red) (day and night) with IASI (blue) (night only) in the tropical belt 20S-20Ns.

6. Interpretation of the annual statistics

6.1 Time profiles of the proxies over 3 years

Plots of the time profiles for various proxies are given in Figure 8. Monthly means of maximum temperature for cloudfree or all pixels have similar annual variations with a maximum in June-July and a minimum in Dec-Jan., meaning that global climate is fairly dominated by the North hemisphere seasons. This is certainly due to the ratio land/sea in the Northern hemisphere. The mean temperature over the spectra (proxy of OLR) is phased with a value oscillating in a 256-259 K range, to be compared with the 255 K Earth equilibrium temperature. The cycles for the proxy of tropopause or high stratosphere/mesosphere (HS/MS) temperatures are much smoother and quite stable respectively at 215 and 243K, the last showing opposite cycle with respect to the surface. The global monthly mean sea surface temperature in cloud free conditions is remarkably stable around 295K (Fig. 9). The cycles for tropopause and HS/MS temperature are slightly stronger over the ocean than in general and show opposite cycles. I think you need to place these statistics in the context of prior reports (e.g previous work) and on what might be expected. Also, what is the size of trends expected from models? Are the data stable enough to see expected (small) trends? Some discussion needed here.

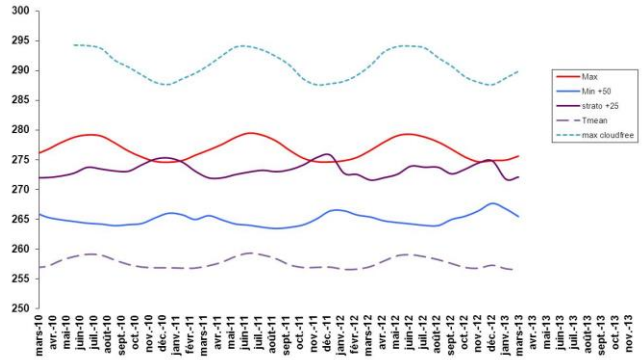

Figure 8: Time series of monthly global means of maximum, minimum (shift of 50K), mean Brightness temperature and temperature at 667.75 cm^{-1} (shifted of 30K) for all pixels (night and day, land and sea)

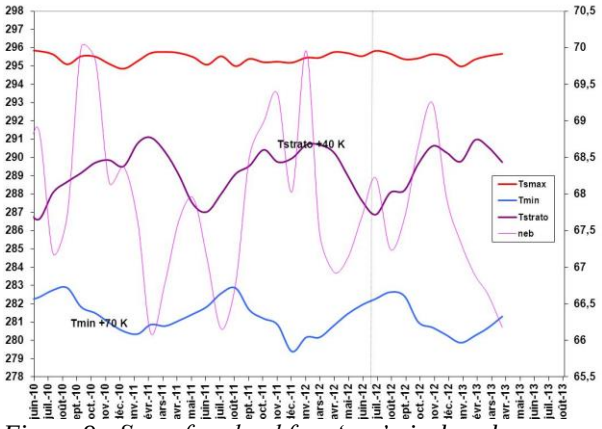

Figure 9 : Same for cloud free 'sea' pixels only

Regarding trace gas variations, as examples the variations of CO and CH_4 are plotted in Fig. 10. The cycles look phased with the surface temperature but with extrema of CH_4 one month later than CO.

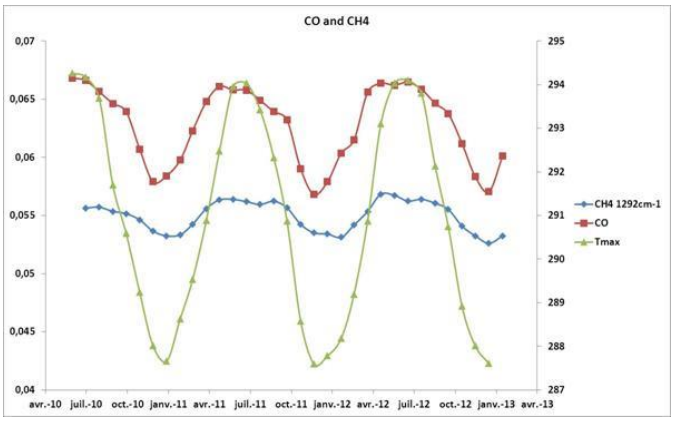

Figure 10: Time series of monthly global means for proxies of CO and CH4 columns in cloud free conditions and comparison with a proxy of surface temperature. How do these compare with SCIMACHY/GOME or AIRS gas climatologies?

6.2 Variations along one year

The month to month variations of global mean spectra along year 2012 have been analysed thoroughly. The seasonal cycle can clearly be showed. Major increase of surface temperature occurs from January to June with a decrease in the second half. With respect to air temperature, from stratosphere to mesosphere, the maximum temperature is in general in January for all pixels and two months later when considering the sea only. The tropopause temperature (minimum of observed temperature) exhibits very small variations overall, nevertheless a small cycle is present in the sea case with a maximum in September and a minimum in January.

Regarding the total humidity seen in HDO band from 2600 to 2730 cm^{-1}, at night time only or at 1243 cm^{-1},the months where total humidity is high are March –April with a minimum in January. The same result is seen for the 'sea' case.

6.3 Gradients month to month

Differences between successive months for spectra of cloud free pixels for all surfaces have been plotted. Consideration of the 4 regions of the spectra: 645-700, 800-1000, 1700-1900 and 2500-2760 cm^{-1} gives information on the gradients of surface temperature, stratospheric temperature and mean humidity.

The minimum and maximum gradients are observed in 2012 for the 4 spectral regions showing that 2012 is more contrasted than 2011. In 2012, a period when the gradients of surface temperature (Ts) and atmospheric humidity (qa) are weak is June-July. For both, they are strongly negative in May-June and positive from August to November. For the stratosphere temperature, the gradients are stronger in 2012 than in 2011. The most negative are from December to February and more positive from September to November. Maybe add a Table here like the others (e.g. Tables 1 and 2), showing what spectral regions correspond to various variables?

6.4 Comparison of interannual anomalies

Anomalies are computed by subtracting average spectra in cloudfree conditions from June 2011 to November 2012. A mean spectrum for the reference period has been computed. With 33 months in the data, the average spectrum is quite stable. Incrementing the climatology each month with data of the month brings marginal change to the mean value. This mean is chosen as 'baseline year' with respect to which anomaly are computed.

Month by month plots are shown on figure 11. The oscillation around the mean is clearly seen: warmer in summer, colder in winter and even in Fall and Spring. Overall, spectra are very close to each other except November 2010. However small discrepancies exist in some limited spectral regions. For instance in March 2012 the brightness temperature in window regions is higher than 2011, but similar in January and February. Temperature in windows for summer 2010 is warmer than 2011 or 2012, while in fall there is a balance between the two first months where 2012 and 2011 are warmer than 2010. Also in the CO_2 bands near 670cm^{-1}, the discrepancies are generally small except in July, November and December with 2010>2012>2011. The brightness temperature here is a proxy of the high stratosphere/mesosphere temperature. The spectra in the water vapour band exhibit small differences except in November.

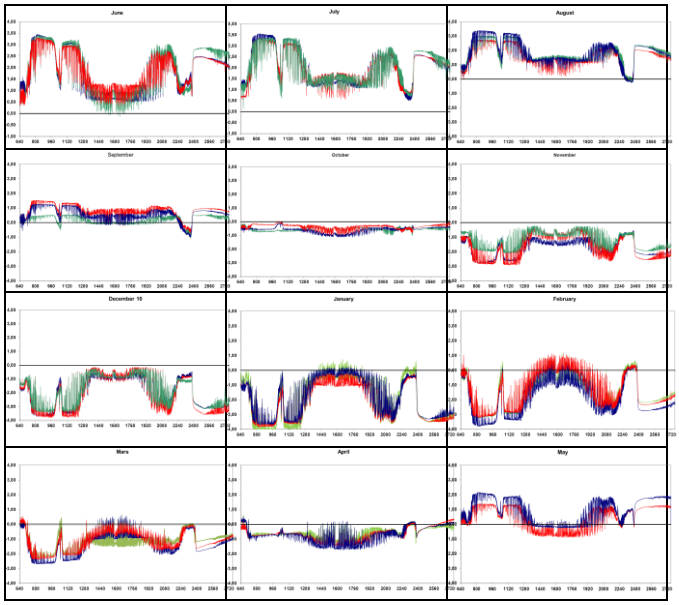

Figure 11 : Spectra for summer months: June, July August (line1), Fall : September, October, November (Line2), Winter : December, January, February (Line 3) and Spring: March, April, May (Line 4). 2010 is dark green, 2011 in red, 2012 in blue and 2013 in light green.

6.5 Inversion of mean annual global variables

Simulations performed with Tigr 2000 atmospheres were compared to the mean annual global spectra in cloud free conditions. The best fit is obtained with the Tigr atmosphere #1050, which is used then to get the Jacobians with respect to the major variables.

Full year (Jan to Dec) averaged spectra have also been computed for years 2011, 2012 and 2013.

Also the differences year to year have been inferred. As an example interannual variation of spectra 2012-2011 is plotted in Figure 12.

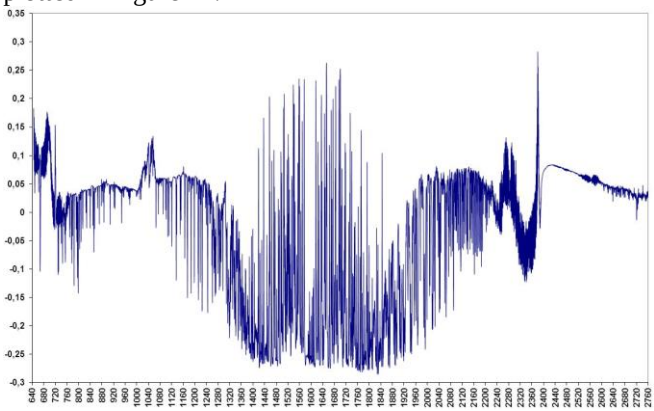

Figure 12: Difference of mean annual IASI spectra from 2012 and 2011 (year from January to December) for cloud free conditions

This plot is obtained for cloud free situations only. Inversion of the parameters have then been performed using a very simple model based on Taylor 's series approximation. The coefficients used in the equations are derived from the sensitivity to each variable (Jacobians) as given by the simulated values obtained for atmosphere 1050. The results of inversion are given in Table 3.
It can observed that the slight increase of surface temperature and troposphere temperature is well retrieved. The decrease of stratospheric temperature is stronger with IASI. It can also be noticed the slight increase of CH_4 and N_2O while O_3 decrease in 2012.

ECV	Ts (K)	Ta LT	Ta LS/MS	H (%)	CO_2 %	O_3 %	CO %	CH_4 %	N_2O %
2012-2011 IASI	0.04	0.12	-1.0	4	0.96	-0.3	0.4	1.3	1.3
2012-2011 NCDC	0.05 (SST)	0.16	-0.42						

Table 3: Comparison of results from inversion of global annual gradients in IASI spectra and NCDC figures from 2011 to 2012

The good comparison between the results and those given by NCDC statistics (http://www.ncdc.noaa.gov/sotc/global/2012/13#gtemp) shows than the proxies from IASI spectra give reliable trends and can be considered as pertinent indicators for climate monitoring.

7. Interannual and seasonal variability

Within one year, it is clear that at global scale for cloudfree land and sea pixels the warmest months are June-July, the coldest are December-January.
Considering 'all pixels' case, the variations are phased with the cloudfree case but with temperature about 15 K lower.
Now for only cloudfree sea pixels the surface temperature remains very stable along the months with less than 1K variations between January and July. The global variations on the Earth are thus dominated by the continental areas, hence by seasonal variations of the northern hemisphere where sea occupies less surface.
Considering the cloud cover the annual cycle has two maxima, the higher is in November, the lower in June. The minima are in September and March. Regarding the total column of water vapour the maximum is in April and the minimum in January.
Generally if surface temperature variations can reach 7 K , the variations for the precursor of tropopause are very slight (less than 2K) and the same for the proxy of the high stratosphere.
The mean monthly spectra for cloudfree conditions were compared month after month to analyse when in the year a discrepancy between years occurs. Clearly the critical month is April or May.

8. Conclusions

Global monthly statistics of IASI radiances for cloud free pixels are very worthy data in climate monitoring studies. They give access to measurements noisy or contaminated unexploited up to now. Regional statistic provide information that has previously been either quite noisy or contaminated.
The statistics are very simple but already contains much information on the planet Earth. The proxies derived from them are very self-consistent showing clear cycles in the year and year to year variations which look in a fair agreement with what is expected. The stability of mean global ocean temperature in cloud free regions is remarkable. So it is for the mean cloud fraction. Inversion has been performed to get year to year gradients for 8 variables (or proxies of these variables) gives figures which are pretty similar to those extracted from NCDC. Such statistics established for regional studies also give interesting results. Over tropical oceans the total water vapour column is very well correlated to the sea surface temperature. Estimate of the sea surface temperature at night gives a fairly reliable ENSO index in the ENSO34 region. IASI allows us to study how variables change in consistency with ENSO events and in particular how water humidity and cloud cover change in accordance.

References

Brindley HE, Harries JE, 2003: Observations of the infrared outgoing spectrum of the Earth from space: The effects of temporal and spatial sampling, J. Climate, 2003, Vol:16,Pages:3820-3833,ISSN:0894-8755(publication doi)

Brindley HE, Allan RP, 2003: Simulations of the effects of interannual and decadal variability on the clear-sky outgoing long-wave radiation spectrum, QJRMS, Vol:129, Pages:2971-2988, ISSN:0035-9009(publication doi)

Article de Tony Slingo sur le changements du climat en fonction du spectre dans notre model de l'epoque: http://onlinelibrary.wiley.com/doi/10.1002/qj.4971235380 3/abstract

Hilton et al.Raymond Armante, Thomas August, Chris Barnet, Aurelie Bouchard, Claude Camy-Peyret, Virginie Capelle, Lieven Clarisse, Cathy Clerbaux, Pierre-Francois Coheur, Andrew Collard, Cyril Crevoisier, Gaelle Dufour, David Edwards, Francois Faijan, Nadia Fourr ié, Antonia Gambacorta, Mitchell Goldberg, Vincent Guidard, Daniel Hurtmans, Samuel Illingworth, Nicole Jacquinet-Husson, Tobias Kerzenmach er, Dieter Klaes, Lydie Lavanant, Guido Masiello, Marco Matricardi, Anthony McNally, Stuart Newman, Edward Pavelin, Sebastien Payan, Eric Péquignot, Sophie Peyridieu, Thierry Phulpin, John Remedios, Peter Schlüssel, Carmine Serio, Larrabee Strow, Claudia Stubenrauch , Jonathan Taylor, David Tobin, Walter Wolf, and Daniel Zhou, 2012: Hyperspectral Earth Observation from IASI: Five Years of Accomplishments, Bull. American met.Soc., March 2012, P347-370

Chalon, G., F. Cayla, and D. Diebel, 2001: IASI: An advanced sounder for operational meteorology. *Proc. 52nd Congress of IAF*, Toulouse France, CNES. [Available online at http://smsc .cnes.fr/documentat ion/ IASI/Publications /PRESENTATION_IAF_2001.pdf.]

Blumstein, D., B. Tournier, F. R. Cayla, T. Phulpin, R. Fjortoft, C. Buil, and G. Ponce, 2007: In-flight performance of the Infrared Atmospheric Sounding Interferometer (IASI) on METOP-A. *Atmospheric and Environmental Remote Sensing Data Processing and Utilization III: Readiness for GEOSS*, M. D. Goldberg et al., Eds., International Society for Optical Engineering (SPIE Proceedings, Vol. 6684)**,** 66840H, doi:10.1117/12.734162 .

Chaumat, L., N. Decoster, C. Standfuss, B. Tournier, R. Armante and N. A. Scott (2006) 4A/OP Reference Documentation, NOV-3049-NT-1178-v3.4, NOVELTIS, LMD/CNRS, CNES, 261 pp.

Stubenrauch, C. J., W. B. Rossow, S. Kinne, S. Ackerman, G. Cesana, H. Chepfer, L. Di Girolamo, B. Getzewich, A. Guignard, A. Heidinger, B. Maddux, P. Menzel, P. Minnis, C. Pearl, S. Platnick, C. Poulsen, J. Riedi, S. Sun-Mack, A. Walther, D. Winker, S. Zeng, G. Zhao, 2012: ASSESSMENT OF GLOBAL CLOUD DATASETS FROM SATELLITES: Project and Database initiated by the GEWEX Radiation Panel, Bull. Amer. Meteor. Soc., doi: 10.1175/BAMS-D-12-00117.

http://www.ncdc.noaa.gov/sotc/global/2012/13#gtemp